An Algorithm for Optimizing Stepper Performance Through Image Manipulation

Chris A. Mack
Department of Defense
Fort Meade, MD 20755

ABSTRACT

The advent of flexible steppers, allowing variation in the numerical aperture, partial coherence, and possibly other optical parameters, allows new opportunities for optimization. This paper will discuss a method for picking the optimum numerical aperture and partial coherence for a given mask pattern and focus budget. An algorithm will be proposed for finding the optimum values. This algorithm could be used as a controller for an intelligent stepper.

INTRODUCTION

A trend is emerging in optical step-and-repeat equipment toward greater flexibility and user control. The latest offering from Ultratech Stepper incorporates a variable numerical aperture objective lens (ranging from 0.2 to 0.4) with variable partial coherence of the illumination [1]. Scanning projection printers from Perkin-Elmer have long been able to pick among many possible wavelength ranges. The new Micrascan I, the first machine to employ the long awaited "step-and-scan" technology, brings the possibility of variable wavelength to stepper technology [2]. The use of excimer lasers as the light source for deep-UV steppers brings with it the potential for generating an arbitrarily shaped illumination source by scanning the laser in the desired shape [3].

It is the goal of this paper to investigate the potential advantages of using flexible steppers for "image manipulation," that is, varying the aerial image of a given mask pattern by varying the optical parameters of the stepper. Obviously, the purpose of image manipulation is to improve the lithographic process in some way. Thus, the first step will be to define some metric or metrics of image quality that can be related directly to lithographic quality. Next the available optical parameters will be varied and the conditions which give the best image (i.e., the maximum value of the image metric) will be found. The three variables that will be used to manipulate the image will be the objective lens numerical aperture (NA), the partial coherence of the illumination (σ), and the shape of the illumination source.

AERIAL IMAGE BEHAVIOR

In previous work [4,5], the advantages and disadvantages of various metrics for image quality were discussed. It was shown that the slope of the log of the aerial image (called the log-slope) is directly proportional to the gradient of photoactive compound and the relative gradient of development rate. Through these relationships, the log-slope is the dominant feature of the aerial image which determines exposure latitude. In general, the value of the log-slope at the mask edge is sufficient to characterize the image. Another metric which is appropriate for spaces and line-space pairs is the ratio of the maximum intensity (usually the center of the space) to the intensity at the mask edge. This ratio is instrumental in determining the sidewall angle of the resist profile. Thus, the two potential metrics are

$$\frac{\delta \ln I}{\delta x} \quad \text{and} \quad \frac{I(center)}{I(edge)} \tag{1}$$

This work uses the log-slope as the image metric. To begin, the behavior of this metric will be investigated as a function of several imaging variables. In any physical system with more than two variables, the key to understanding the behavior of the system lies in choosing an appropriate graphical representation of the data. A good choice of graphs can make complicated behavior easy to visualize. Several graphs will prove useful for understanding image behavior including the log-slope versus linewidth curve, the log-slope versus numerical aperture, and the log-slope defocus curve.

The log-slope linewidth curve shows the effect of increasing linewidth on the quality of the aerial image. Intuitively, one would expect that increasing linewidth would improve the image quality, leveling off at some value for very large features. In fact, the behavior is

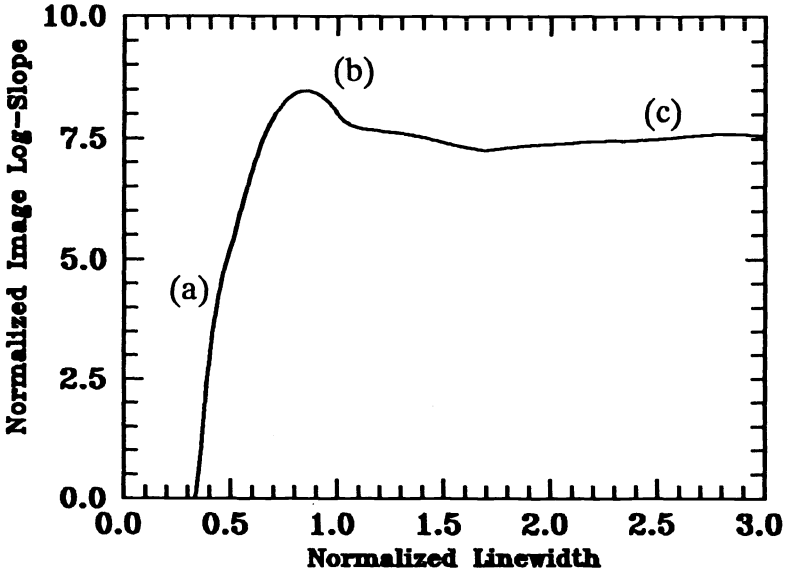

Figure 1: Log-slope linewidth curve (σ = 0.5, equal lines and spaces).

somewhat more complicated. A plot of normalized log-slope versus normalized linewidth is shown in Figure 1 for equal lines and spaces and a partial coherence of 0.5. There are three regions to this curve. Region (a) corresponds to high resolution features and is thus called the high resolution region. As expected, the image quality increases almost linearly with linewidth. In the low resolution region (c), the log-slope levels off as expected to a value corresponding to an isolated edge. In the medium resolution region (b), however, the behavior is less than obvious. Here, the effects of coherence cause the image log-slope to peak at about k=0.85. The origins of this behavior have been explained previously [6].

The effect of defocus on the image can be shown in a log-slope defocus curve [5]. This curve shows the degradation of image quality as the image goes out of focus. Figure 2 shows three log-slope defocus curves corresponding to a given linewidth and three different numerical apertures. The important feature of Figure 2 is that the curves cross. When deciding on the best value of NA for this linewidth, one must specify the focal range for which the line is to be printed. If a DOF range of ±2 microns or less is required, the high NA lens is definitely preferred. However, higher amounts of defocus show that the lower NA lenses may give better results. Another way to view this effect is to plot log-slope versus NA for different amounts of defocus, as shown in Figure 3. One can see that the optimum value of NA depends on the amount of defocus.

Using the three types of curves described above, it is possible to characterize the effects of variable optical parameters on the image. In general, the optimum set of conditions will depend on the amount of defocus specified. This amount corresponds to the total amount of focus errors built into the process (i.e., the focus budget). Focus budgets of ±1.0 to ±1.5 microns are typical [7].

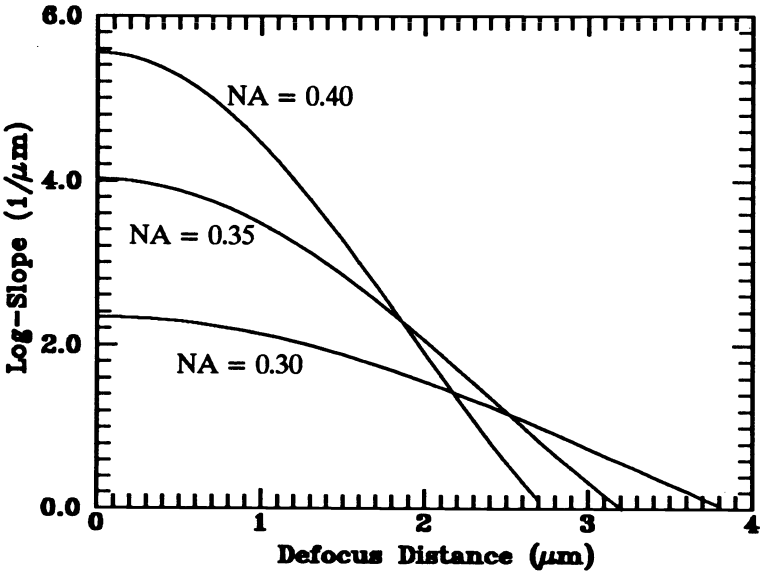

Figure 2: Effect of numerical aperture on the log-slope defocus curve (0.6 μm lines and spaces, g-line, σ=0.5).

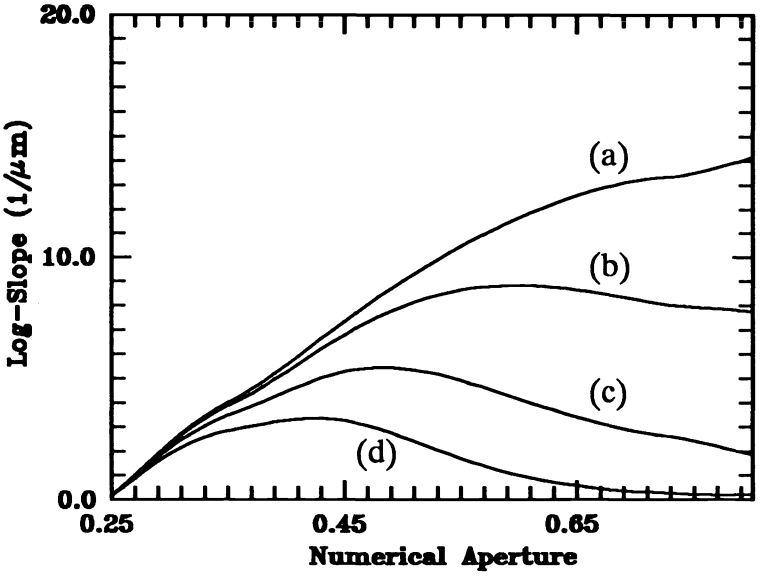

Figure 3: Log -slope versus numerical aperture (0.6 μm lines and spaces, g-line, σ=0.5) for (a) in-focus, (b) 0.5 μm defocus, (c) 1.0 μm defocus, and (d) 1.5 μm defocus.

IMAGE MANIPULATION

The concept of image manipulation involves answering the following question: For a given feature size and focus budget, what are the optimum optical parameters? To be more specific, consider a hypothetical g-line stepper with a variable NA in the range of 0.24 to 0.7, and a partial coherence that can vary between 0.1 and 0.9. Assuming focus budgets of ±1.0 and ±1.5 microns, what are the optimum NA and σ for a variety of different feature types and sizes? Examining Figure 3, one can see that the optimum NA for these 0.6 micron line-space pairs is significantly different for the two focus budgets of interest (curves (c) and (d)). By generating multiple curves like Figure 3 for different linewidths and partial coherences, the optimum optical parameters can be determined within the range of our hypothetical stepper.

Figures 4 through 15 show contour plots of the image log-slope as a function of numerical aperture and partial coherence. Figures 4 and 5 show the contours of log-slope for 0.5 μm lines and spaces with 1.0 μm and 1.5 μm of defocus, respectively. There is a very distinct optimum in each plot: NA = 0.52 and σ = 0.67 for 1.0 μm defocus, and NA = 0.41 with σ = 0.82 for 1.5 μm defocus. There is a general trend that the optimum NA decreases and the optimum coherence factor increases as defocus increases. As a simple rule of thumb, a typical photoprocess will require a minimum log-slope of about 5 μm^{-1}. Thus, a half-micron process on our hypothetical g-line stepper is quite marginal, as one would expect. Note also that the spacing of the contour lines is smaller on the low-NA side of the optimum, thus an error on the high-NA side causes less degredation. Also, near the optimum the log-slope varies slowly with partial coherence.

Figures 6 and 7 show a very common phenomenon. At 1.0 μm defocus, the optimum point is NA = 0.41 with σ = 0.1 (the lowest value for our stepper). However, when the amount of defocus is increased to 1.5 μm, the value of the log-slope at this point drops by a factor of 5. Although this point is the mathematical maximum of the 1.0 μm defocus data, it is not a very "optimal" operating point if there is any chance the focus error can increase. A more reasonable value may be NA = 0.45, σ = 0.5. These figures show the importance of determining a realistic focus budget before finding the optimum image settings.

As the feature sizes get larger there is less reason to have a high NA stepper. For the 0.7 μm lines and spaces depicted in Figures 8 and 9, the optimum NA remains below 0.4. Again the optimum partial coherence increases as the defocus increases (it goes to 0.7 for 2.0 μm defocus).

As expected, the isolated lines of Figures 10-15 show improved log-slopes over the corresponding equal lines and spaces. The maximums are broader, but are at roughly the same positions. There is also less chance of a dramatic drop in log-slope with defocus for isolated lines. The contours are in general spaced farther apart than for the packed features.

ALGORITHM FOR IMAGE MANIPULATION

All of the above results were obtained using the general lithography simulator PROLITH/2 [8] running on an IBM PC compatible. Although the exact details of the aerial image model used in PROLITH/2 have not been published, it is based on an extended source method. A simple variation of this method could be used to quickly and efficiently calculate only the log-slope of the aerial image at the mask edge. Contour plots such as the ones shown here can be generated in a few seconds. Standard response surface techniques can be implemented to easily find the optimum operating point. The result is a real time method of determining the preferred stepper parameters for a given mask feature and focus budget. The mathematical details of this algorithm will be released at a later date.

As was shown earlier, it is critical to have a realistic estimate of the focus budget for a process in order to find the optimum stepper parameters. It is also important to know the aberration characteristics of the stepper being used. All optical lithography exposure tools suffer from image degradation due to lens aberrations - the only question is to what degree. Simulation techniques exist to describe the effects of aberrations on the log-slope of the image once the characteristics of a projection system are known. Determining these characteristics is not an easy matter. An accurate means of image monitoring (i.e, actually measuring the aerial image of a stepper) is required to fully characterize a stepper and thus take full advantage of the technique of image manipulation.

CONCLUSIONS

The present and future availability of flexible steppers affords a new level of optimization in the lithographic process. The ability to vary the numerical aperture and the

size and shape of the illumination source will allow optimization of the aerial image for a given feature size and focus budget. As Figures 4 through 15 indicate, there is no one set of optimum conditions for all features and focus budgets. Since the manufacture of integrated circuits entails the use of many different lithography steps with many different geometries and topographies, a flexible stepper could improve the quality of each lithography step through image manipulation. The algorithm described in this paper could be the controller for an intelligent stepper of the future.

REFERENCES

1. A. C. Stephanakis and D. I. Rubin, "Advances in 1:1 Optical Lithography," *Optical Microlithography VI, Proc.*, SPIE Vol. 772 (1987) pp. 74-85.

2. J. D. Buckley and C. Karatzas, "Step and Scan: a Systems Overview of a New Lithography Tool," *Optical/Laser Microlithography II, Proc.*, SPIE Vol. 1088 (1989) pp. 424-433.

3. V. Pol, et al., "Excimer Laser-based Lithography: a Deep Ultraviolet Wafer Stepper," *Optical Microlithography V, Proc.*, SPIE Vol. 633 (1986) pp. 6-16.

4. C. A. Mack, "Photoresist Process Optimization," *KTI Microelectronics Seminar, Proc.*, (1987) pp. 153-167.

5. C. A. Mack, "Understanding Focus Effects in Submicron Optical Lithography," *Optical/Laser Microlithography, Proc.*, SPIE Vol. 922 (1988) pp. 135-148, and *Optical Engineering*, Vol. 27, No. 12 (Dec. 1988) pp. 1093-1100.

6. C. A. Mack, "Optimum Stepper Performance Through Image Manipulation," *KTI Microelectronics Seminar, Proc.*, (1989) pp. 209-215.

7. B. J. Lin, "Paths to Sub-half-micrometer Optical Lithography," *Optical/Laser Microlithography, Proc.*, SPIE Vol. 922 (1988) pp. 256-269.

8. FINLE Technologies, P.O.Box 261034, Plano, Texas 75026.

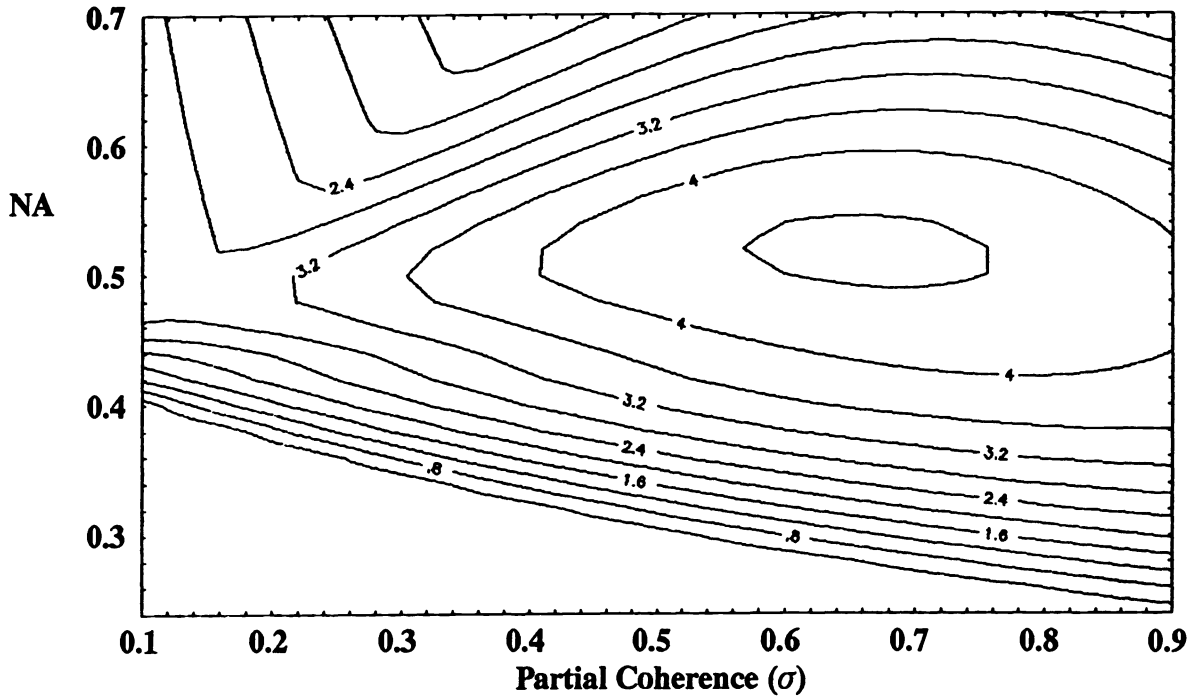

Figure 4: Log-slope contour plot for 0.5 μm line/space with 1.0 μm defocus.

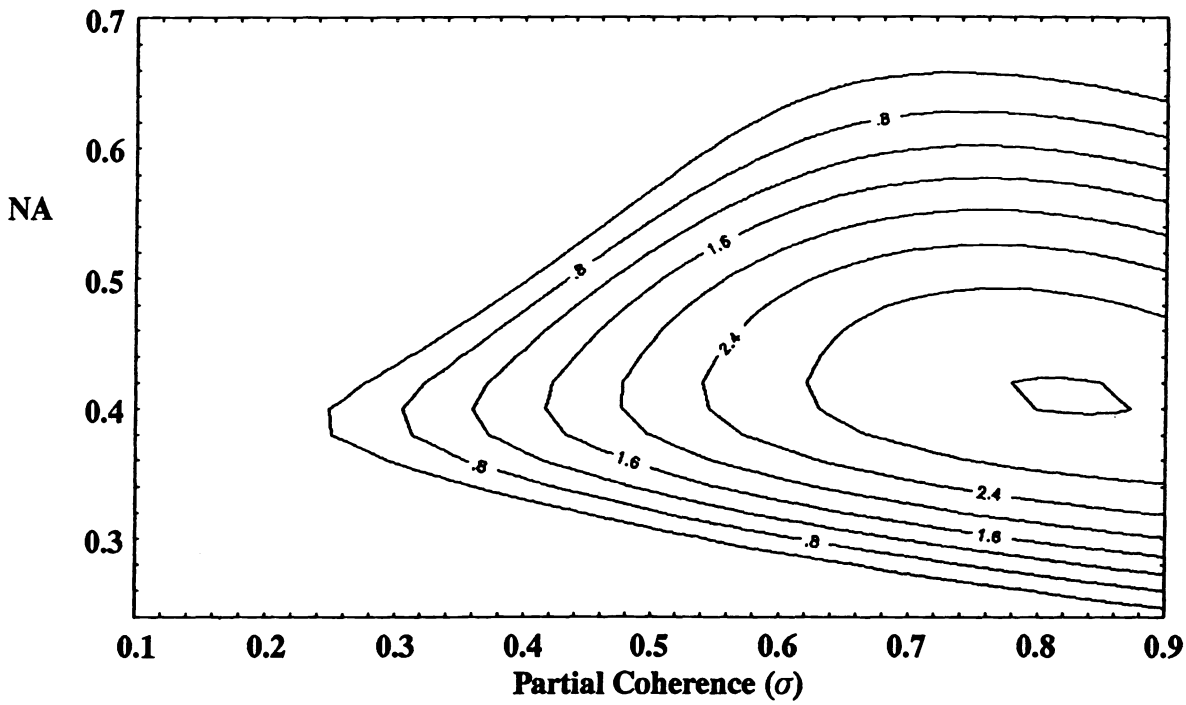

Figure 5: Log-slope contour plot for 0.5 μm line/space with 1.5 μm defocus.

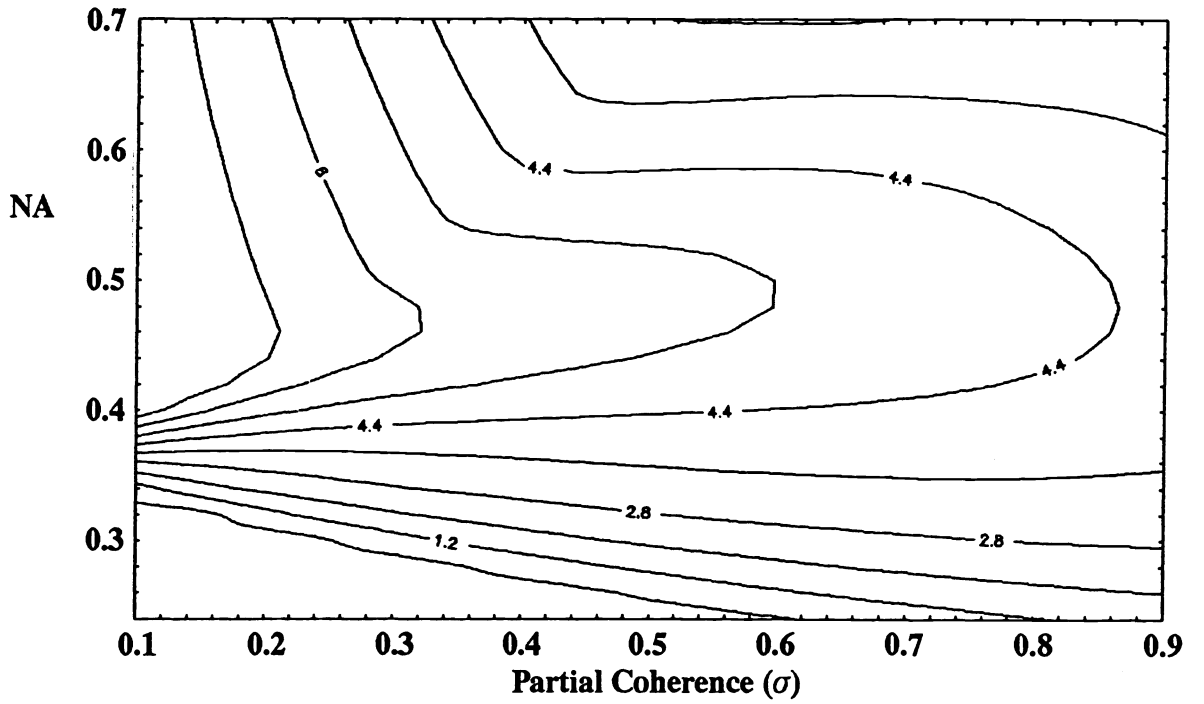

Figure 6: Log-slope contour plot for 0.6 μm line/space with 1.0 μm defocus.

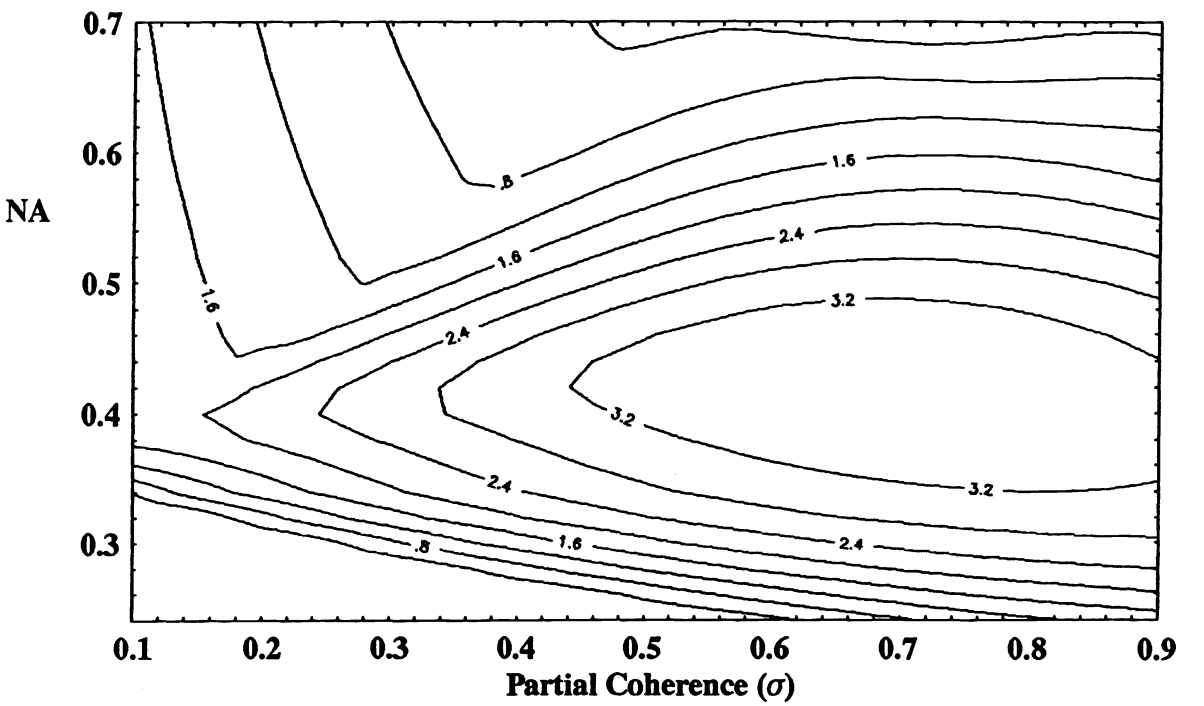

Figure 7: Log-slope contour plot for 0.6 μm line/space with 1.5 μm defocus.

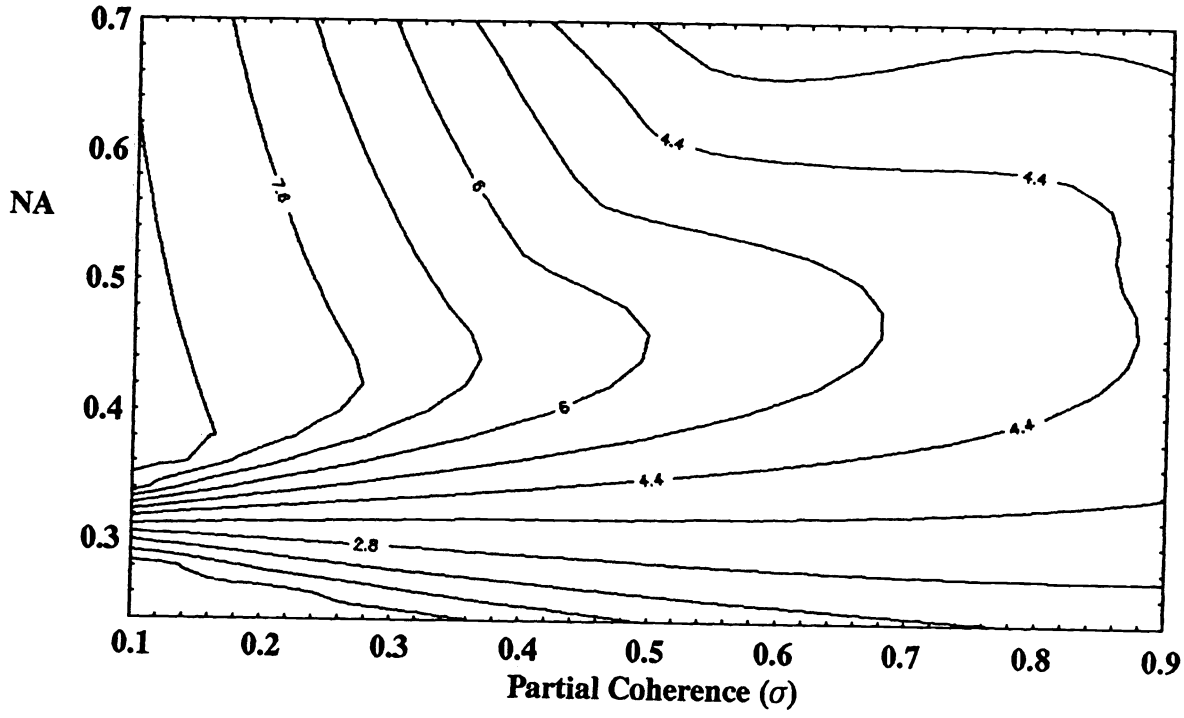

Figure 8: Log-slope contour plot for 0.7 μm line/space with 1.0 μm defocus.

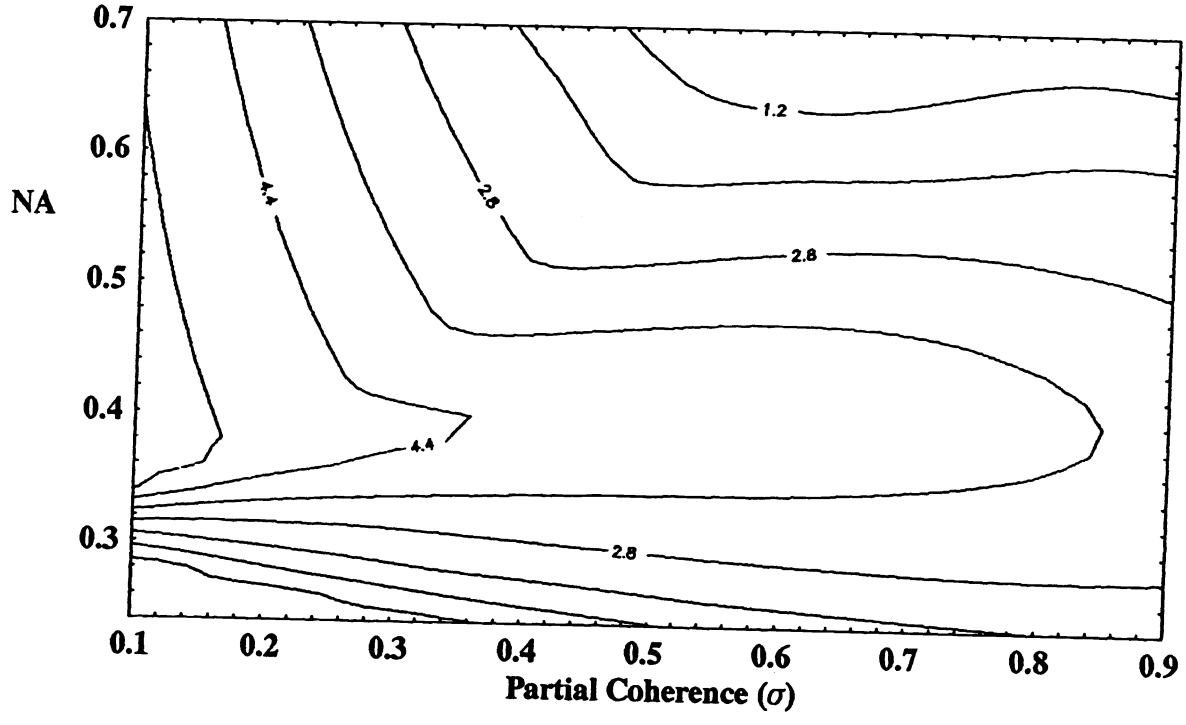

Figure 9: Log-slope contour plot for 0.7 μm line/space with 1.5 μm defocus.

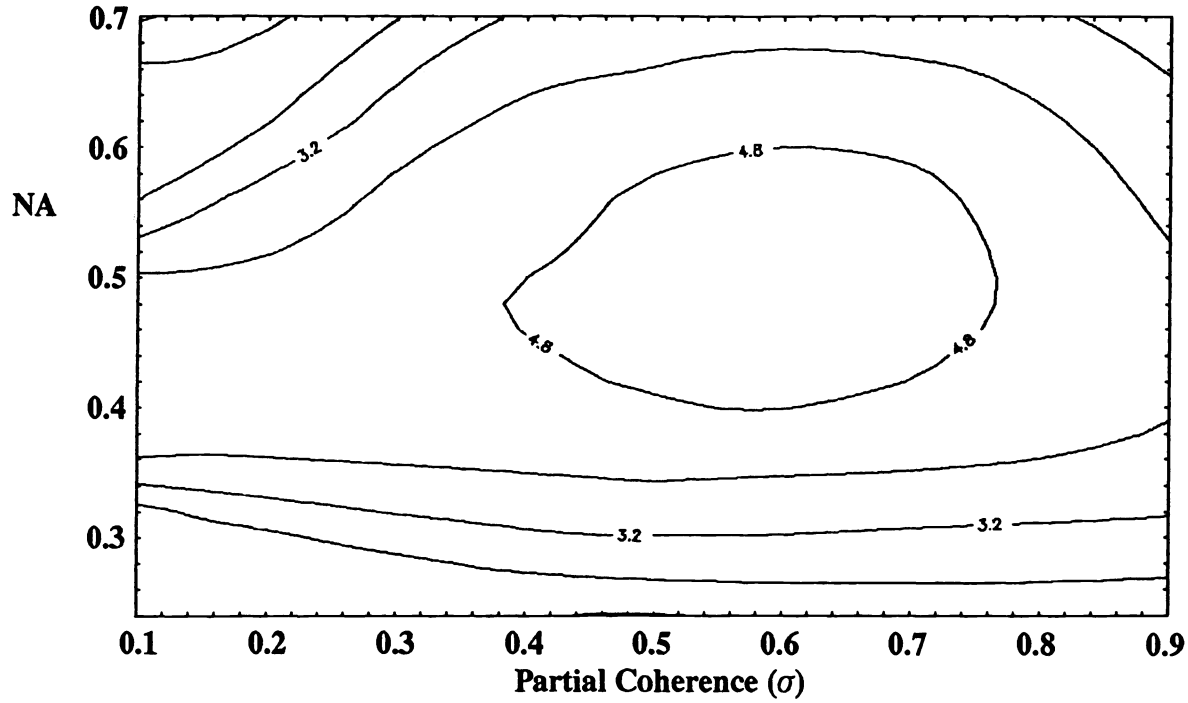

Figure 10: Log-slope contour plot for 0.5 μm isolated line with 1.0 μm defocus.

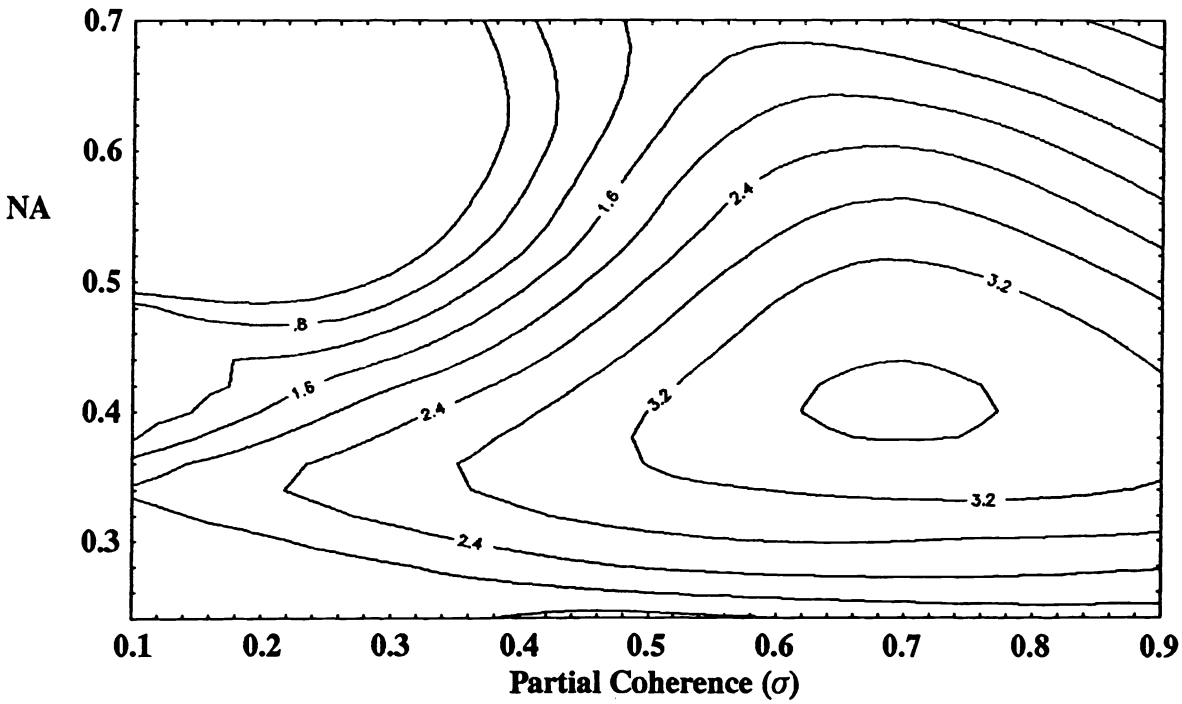

Figure 11: Log-slope contour plot for 0.5 μm isolated line with 1.5 μm defocus.

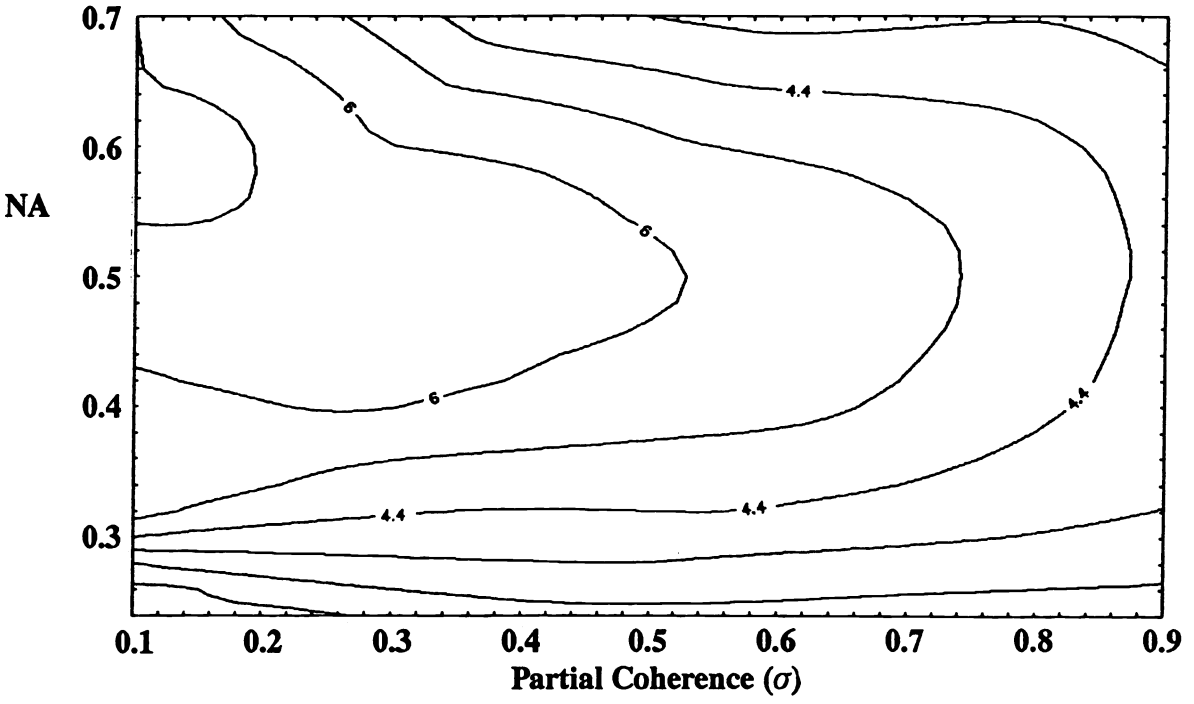

Figure 12: Log-slope contour plot for 0.6 μm isolated line with 1.0 μm defocus.

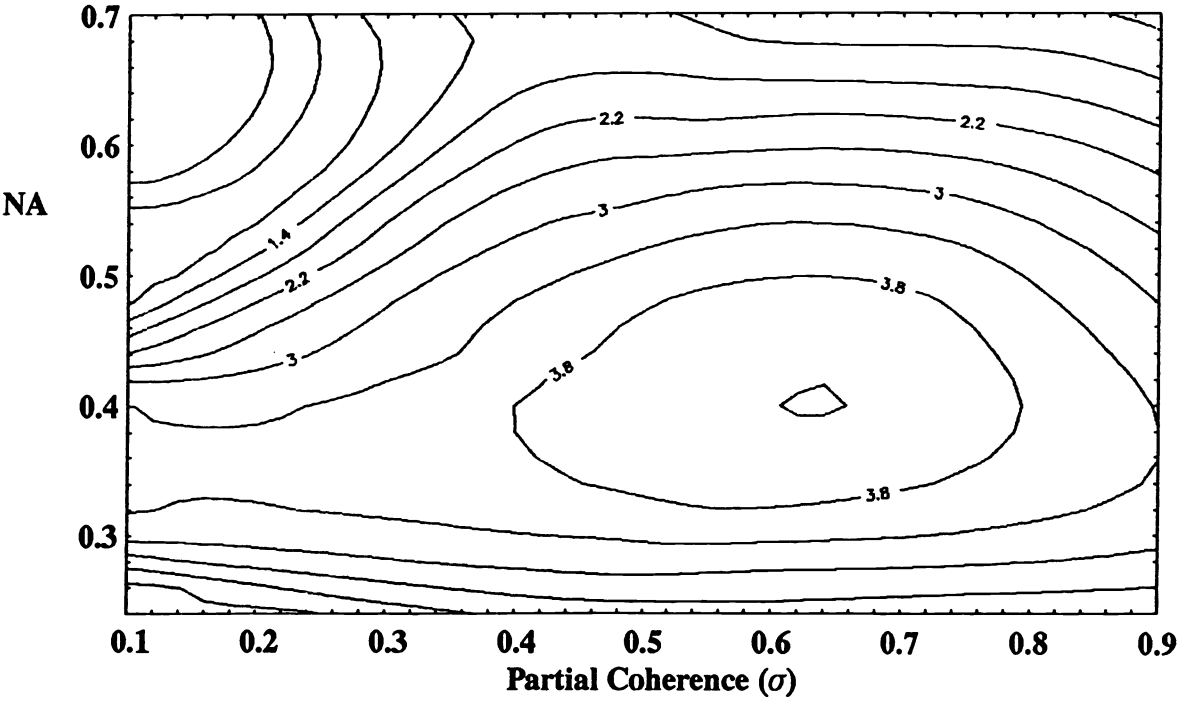

Figure 13: Log-slope contour plot for 0.6 μm isolated line with 1.5 μm defocus.

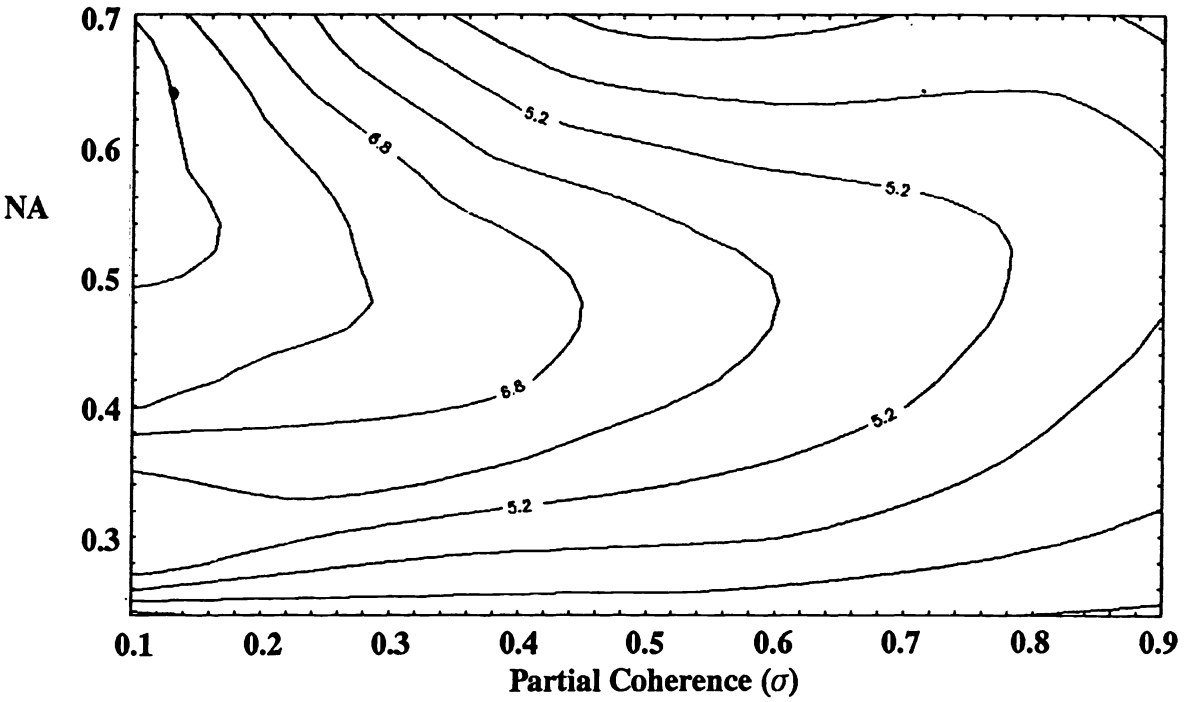

Figure 14: Log-slope contour plot for 0.7 μm isolated line with 1.0 μm defocus.

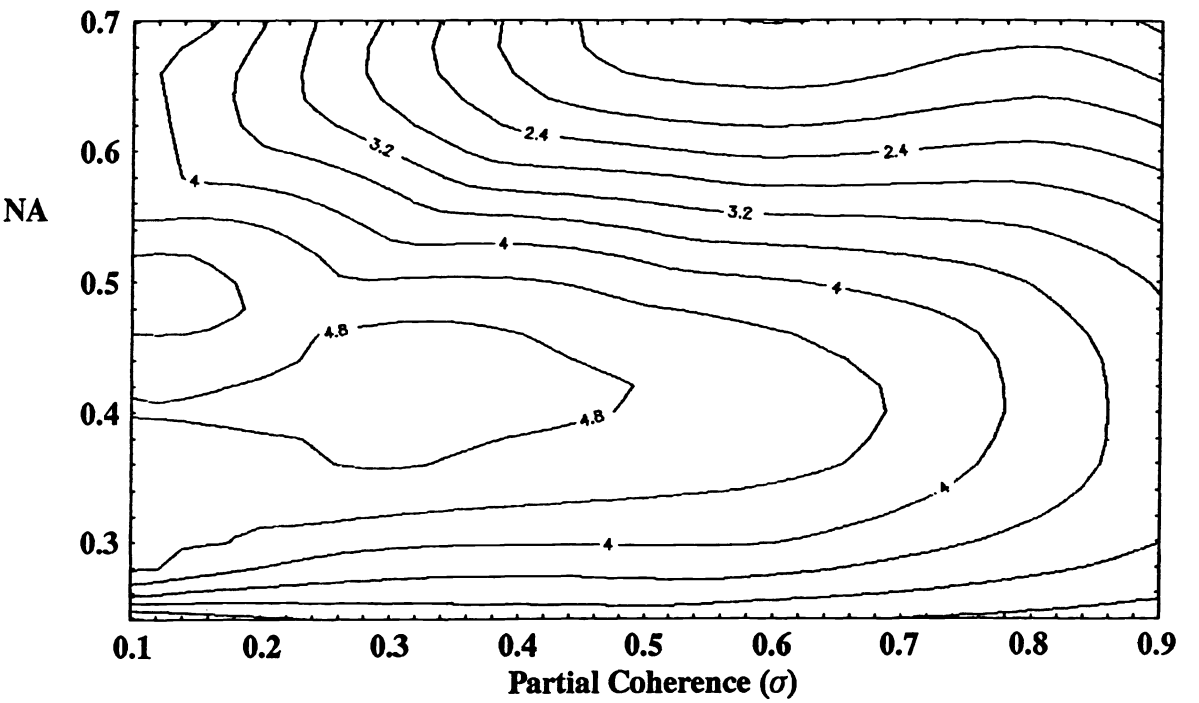

Figure 15: Log-slope contour plot for 0.7 μm isolated line with 1.5 μm defocus.